Title

Conductive Ink with Circular Life Cycle for Printed Electronics

Journal

Advanced Materials, 34(30)

ISSN

0935-9648

Authors

Kwon, Junpyo

DelRe, Christopher

Kang, Philjun

et al.

Publication Date

2022-07-01

DOI

10.1002/adma.202202177

Conductive ink with circular life cycle for printed electronics

Junpyo Kwon, Christopher DelRe, Philjun Kang, Aaron Hall, Daniel Arnold, Ivan Jayapurna, Le Ma, Matthew Michalek, Robert O. Ritchie, and Ting Xu*

J. Kwon
Department of Mechanical Engineering, University of California, Berkeley, CA 94720, USA
Materials Sciences Division, Lawrence Berkeley National Laboratory, Berkeley, CA 94720, USA

C. DelRe, L. Ma
Materials Sciences Division, Lawrence Berkeley National Laboratory, Berkeley, CA 94720, USA
Department of Materials Science and Engineering, University of California, Berkeley, CA 94720, USA

P. Kang
Department of Chemistry, University of California, Berkeley, CA 94720, USA

A. Hall, I. Jayapurna, M. Michalek
Department of Materials Science and Engineering, University of California, Berkeley, CA 94720, USA

D. Arnold
Department of Chemical Engineering, University of California, Berkeley, CA 94720, USA

R. O. Ritchie
Department of Mechanical Engineering, University of California, Berkeley, CA 94720, USA
Materials Sciences Division, Lawrence Berkeley National Laboratory, Berkeley, CA 94720, USA
Department of Materials Science and Engineering, University of California, Berkeley, CA 94720, USA

T. Xu
Materials Sciences Division, Lawrence Berkeley National Laboratory, Berkeley, CA 94720, USA
Department of Materials Science and Engineering, University of California, Berkeley, CA 94720, USA
Department of Chemical Engineering, University of California, Berkeley, CA 94720, USA

Keywords: recycle; transient electronics; 3d printing; enzyme mixtures; polymer composite

Citation: J. Kwon, C. DelRe, P. Kang, A. Hall, D. Arnold, I. Jayapurna, L. Ma, M. Michalek, R. O. Ritchie and T. Xu, "Conductive Ink with Circular Life Cycle for Printed Electronics", *Advanced Materials*, vol. 34 (3), July 2022, art.# 2202177; doi.org/10.1002/adma.202202177.

Abstract: Electronic waste rivals the energetic cost and environmental burden of plastic waste due to the rarity and toxicity of the heavy metals used. Here, we introduce recyclable conductive composites for printed circuits formulated with polycaprolactone (PCL), conductive fillers, and enzyme/protectant nanoclusters. These inks are degraded by immersion in warm water and their functional fillers can be recovered at ~94% without compromising device performance, storage, or robustness. Circuits can be printed with good flexibility (breaking strain ~80%) and conductivity (~2.1 $\times$ 10^4 S/m). The circuit disintegration can be programmed by thermal treatment to meet stability demands during operation. The printed circuits remain functional and degradable after at least 7-month shelf storage at room temperature and one month of continuous operation under electrical voltage. The present studies demonstrate a feasible approach to developing recyclable and easily disposable printed electronics for applications such as wearable electronics, biosensors, and soft robotics.

Main Text

Unrecycled materials at the end of their life impose a significant environmental and economic burden due to pollution buildup and loss of valuable resources.[1] Given the rapid and increasing turnover rate of electronic products, electronic waste (e-waste) containing toxic substances[2] and precious metals[3] are a pressing environmental, safety, and economic concern.[4] Yet, recyclability of electronics is rarely a design criteria, and existing recycling procedures lead to secondary pollution and insufficient recovery of precious components.[5]

Biologically resorbable electronics, called transient electronics[6], have controllable operational lifetimes and on-demand response upon being triggered.[7] In such electronics, extra protection layers are used to ensure stable operation during usage. However, they are stimuli-sensitive to environmental conditions, such as heat, moisture, pH, acids, ion species, UV lights, etc.,[8] which requires additional fabrication steps and increases recycling costs. Recently, embedding enzyme nanoclusters[9] has shown to be effective in programming the degradation of polyesters. Therefore, composite materials that integrate these developments may serve as the ideal entry point toward sustainable printed electronics and e-waste reduction.

Degradable composites can provide a suitable material platform to develop conductive inks **(Schematic 1)**. Here, we have fabricated a flexible electronic circuit using a composite whose polymer binder is selectively depolymerized by embedded enzymes. The ink is mechanically robust (tensile strength ~6.3 MPa) exhibiting good mechanical flexibility (strain at break ~80%) and electrical conductivity (~2.1 × 10^4 S/m). The circuit's degradation is triggered with only warm water (37-41˚C) and the metal fillers can be collected and reused with no observable functional loss. Thermal treatment can be used to program the degradation rate and modulate device operation. A non-purified BC-Lipase with impurities is used to formulate conductive ink as opposed to a purified enzyme.[9c] The circuits remain fully functional and degradable after 7-months storage and 1-month continuous operation under 3 V electrical voltage at moderate temperatures with uncontrolled humidity. Furthermore, in the present work we have developed composites using commercial sourced enzymes with undetermined stabilizer, a significant step forward toward scalable device fabrication.

Previous studies in enzyme-containing plastics focused on degradation mechanisms and used purified enzymes.[9a,9c] This significantly limits the scalability and increases cost. Commercially available enzymes are more cost effective but contain undefined stabilizers. Thus, we first focused on developing random heteropolymers (RHPs) to effectively stabilize the enzyme cocktail (BC-Lipase$_{np}$) purchased directly from Sigma-Aldrich®. Analysis showed that the enzyme content was < 1 %, and the further presence of silicon dioxide nanoparticles, as shown in **Figures 1a and S1**. We hypothesized that there are favorable interactions between the enzymes and stabilizers, and therefore RHPs have to compete with these commercial stabilizers. Thus, we first screened RHPs as a function of their molecular weights.

RHP's molecular weight (MW) affects the catalytic performance of BC-Lipase$_{np}$. For instance, low MW RHPs and contaminants influence the morphology of the polymer matrix,

limiting chain-end accessibility of the embedded enzymes which reduces the polymer-to-monomer conversion.[9a] Increasing the molecular weight of the RHP may also lead to multivalency which achieves better RHP-Lipase complexation, enhancing activity retention and dispersion. Thus, RHPs with the same monomer composition but different MWs (68kDa, 81kDa, and 127kDa) were tested. The composite films composed of the PCL and RHP-enzyme complex (PCL/RHP/BC-Lipase$_{np}$) were prepared under the same conditions and immersed in warm water (37˚C) for 24 hours **(Figure 1b)**. The films with 68 kDa RHP exhibited 65.9% (± 8.4%) weight loss for 24 hours. The films with 128 kDa RHP showed 80.0% (± 16.7%) weight loss under the same experimental conditions. Although the films prepared with purified BC-Lipase showed the highest degradation rates displaying 91.5% (± 1.6%) weight loss for 24 hours, the 128 kDa RHP had a better performance and was chosen for subsequent studies **(Figure 1c)**.

Silver (Ag) flakes were blended as a conductive filler to impart electrical conductivity. When Ag/PCL (filler load ~80 wt.%) was mixed with fluorescently labeled RHP/BC-Lipase$_{np}$, fluorescence microscopy confirmed that the enzymes were homogeneously dispersed in the PCL matrix even when high concentrations of the Ag flakes were introduced **(Figure 2a)**. After ~80 hours of immersion in warm water (37˚C), the Ag flakes precipitated to the bottom of the container. The reclaimed Ag flakes showed a morphology similar to the virgin material under the optical microscope (**Figure S5**). Thermogravimetric analysis (TGA) **(Figure 2b)** confirmed that the reclaimed Ag flakes had a purity greater than 94% with less than 6% of organic material absorbed. The process can be repeated multiple times and the conductivity of the ink based on the reclaimed Ag flakes remains similar to that from as purchased material **(Figure 2c)**.

The electrical conductivity of the ink (PCL/Ag/RHP/BC-Lipase$_{np}$) was logarithmically increased as the volume fraction of Ag flakes was increased from 10 vol.% to 30 vol.%

(Figure S6), which is consistent with percolation theory[10] and previously introduced composite studies.[11] Upon further increase of the volume fraction of Ag flakes, the conductivity slightly improved until a plateau was observed at 30 vol.% to 35 vol.%. Cross-sectional scanning electron microscopy (SEM) analysis validated the formation of a continuous conducting network of the Ag flakes. Thus, the optimized ink was formulated with 78.9 wt.% (30 vol.%) Ag flakes. The exhibited conductivity of 2.1×10^4 S/m satisfies the requirements for electronics.[8] The results of uniaxial tensile tests, given in **Figure S7**, show the engineering stress-strain curve of a tensile dog-bone specimen made of the composite (following ASTM Standard D1708). The composite displayed a maximum tensile strength of 6.3 MPa with a tensile ductility, *i.e.* the strain at break, of ~80%. Hence, the composite composed of 78.9 wt.% Ag flakes achieves both electrical conductivity and mechanical robustness.

Chemical and thermal stability is requisite to ensure stable operations during usage.[12] The stabilities of the PCL matrix and the composite ink with high concentrations of Ag flakes (78.9 wt.%) were tested. Fourier transform infrared spectroscopy (FT-IR) was used to confirm the chemical integrity of the PCL binders before and after adding Ag/RHP/BC-Lipase$_{np}$. As shown in **Figure S8**, PCL shows the main characteristic peaks of ester group that appear at 1720 cm^{-1} corresponding to the stretching of C=O and 1294 cm^{-1}, 1240 cm^{-1}, and 1184 cm^{-1} corresponding to the stretching of C–O–C.[13] Such typical peaks were all displayed in the spectra of PCL/Ag/RHP/BC-Lipase$_{np}$ without showing additional peaks or broadening bands.

TGA was carried out at 25˚C to 600˚C to evaluate thermal stability and to confirm the filler ratios used in the selected composite. **Figure S9** shows the weight loss curves of the PCL and PCL/Ag/RHP/BC-Lipase$_{np}$. TGA profiles of the PCL show that thermal degradation of the PCL starts above 370˚C, but was completely decomposed around 400˚C. The composite also began to degrade near 390˚C indicating a weight loss of nearly 80% up to

400˚C. The slight increase of the onset decomposition temperature of the PCL/Ag/RHP/BC-Lipase$_{np}$ indicates that the mobility of polymeric (PCL) chains in the composite is affected by adding the Ag flakes.[14] This also might negatively affect the enzymatic degradability.[9c] To further investigate, differential scanning calorimetry (DSC) was performed to study how the Ag fillers could affect the PCL crystallization. There was a small increase in melting temperature from 58˚C ±1.2˚C to 59˚C ± 0.7˚C. This result indicates that the lamellae thickness of the PCL is insignificantly affected by the Ag flakes **(Figures S10)**.

The degradability of the composites under electric fields was verified to identify any possible denaturation of the enzyme. The enzyme's activity was monitored by the collapse of the percolated metallic filler networks leading to the electrical conductivity loss **(Figure S11)**. **Figure 3a** and **Video S2** show that Ag/PCL does not show any current change, although the conductivity of Ag/PCL/RHP/BC-Lipase$_{np}$ decreases with time. The surfaces of both tested circuits were characterized using SEM **(Figure 3b)**. The circuit without RHP/BC-Lipase$_{np}$ did not show any degradation. However, the circuits based on the PCL/Ag/RHP/BC-Lipase$_{np}$ composite were degraded due to the enzymatic depolymerization of the PCL chains in percolating networks of Ag flakes. The selective biodegradation of PCL chains can be fully employed to recycle different types of fillers. **Figure S12** shows that the applied degradation mechanism is still active under 50 V with carbon black as the conductive filler, which enables the selection of carbon-based conductive particles based on user preferences.

The circuits remained degradable after storage in ambient conditions for seven months, followed by up to 31 days of continuous operation under a load of 3 V **(Figure S13)**. The use of RHPs accounts for the stability and degradability over a long period of time and under electrical voltage. Confining RHP/BC-Lipase$_{np}$ in a polymer matrix increases its stability by restricting the enzyme's translational and conformational mobility. Furthermore,

the operating voltage (3-50 V) is much lower than the voltage (> 5 kV) that affects the forces involved in the 3D structure and conformation of lipase.[15] The size of the enzyme-RHP clusters (hydrodynamic diameter d_h > 300 nm) **(Figure S2)** is larger than the typical electron tunneling distance (a few nanometers),[16] which likely prevents voltage-induced denaturation while the material is in operation.

Stable operation is crucial for transient electronics during usage. By relying on enzyme catalyzed depolymerization to breakdown the circuits, the hydrolysis rate can be controlled by degrading temperature. At temperatures below ~30˚C, no degradation occurs because the hindered enzyme and polymer mobility prevents substrate binding and subsequent depolymerization. Upon increasing the temperature to 41˚C, degradation significantly accelerates as observed from analysis of gel permeation chromatography (GPC) measurements **(Figure 3c)**. This is due to the enhanced chain mobility and thermodynamic driving force for crystalline segments to be "pulled" from their lamellae[9c].

In addition, the chain-end mediated degradation of PCL chains can be controlled by increasing the lamellae thickness of the PCL matrix through thermal annealing. Accordingly, the printed circuit was thermally annealed under 49˚C[9c] for 5 days. As shown in **Figure 3d**, DSC confirms a respective ~10% and ~6˚C increase in crystallinity and melting temperature of the thermally annealed circuits, corresponding to a significantly increased crystalline lamellae thickness which reduced the degradation rate **(Figure 3e)**. The control of crystalline properties of the binder can be exploited to tune degradation rates and preserve latency even in hot and humid operating conditions.

The ink can be printed on a variety of types of substrates, such as glasses, rubbers, living plants, and degradable polyesters **(Figure 4)**. As the printed materials are designed to have mechanical flexibility and electrical conductivity, their mechanical deformation can be detected from monotonic conductivity changes in cyclic stretch tests (1,000 times and 1 cycle/

sec) **(Figure S14)**. The composite can also be fabricated using hot melt extrusion. In this work, the ink was prepared by melt blending of PCL/RHP/BC-Lipase$_{np}$ and 79.8 wt.% Ag flakes at under 60˚C for less than 5 mins. The composite melt can be extruded using a syringe without using any organic solvents. The melt-extruded filament also exhibited good electrical conductivity and degraded when immersed in warm water **(Figure S15)**.

Severe reductions in mechanical and adhesion strengths of the printed circuits after degradation were observed **(Figure S16 and Video S3)**. This weak interfacial bond among the materials can be advantageous for sorting different components[4a], such as circuits, resistors, capacitors, batteries, etc., which are strongly fastened in e-waste.[17] To demonstrate the reduction in adhesion force induced by the degradation of the PCL matrix, we performed lap-shear adhesion tests using flexible and stretchable substrates **(Figure S17a)**. The composite ink was evenly spread (5 × 5 mm) on one elastomer substrate and another elastomer was pressed to form a lap junction. A set of the joints were immersed in warm water for 12 hours and then dried overnight under ambient conditions. During the tests, a strong adhesion of the as cast ink was observed with the failure force and displacement estimated to be 9.4 N (± 1.0 N) and 18.2 mm (± 5.0 mm), respectively. In contrast, adhesion strength and displacement at failure significantly decreased to 6.5 N (± 0.8 N) and 5.7 mm (± 2.6 mm), respectively. All of the failures were characterized as cohesive failures and a few defects could be identified from the fracture surfaces **(Figure S17b)**, indicating that the significant reduction in adhesion force was due to the degradation of the PCL matrix.

In summary, non-purified BC-Lipase/RHP complexes were incorporated into Ag/PCL composites, which catalyze the hydrolytic degradation of PCL chains in both film and printed states upon immersion in warm water. This RHP-assisted enzymatic depolymerization enables easy separation of system components and recycling of functional particles even after months of storage and use under ambient conditions. Furthermore, polymer degradation rates can be

controlled by temperature and post-heat treatment after direct ink writing or melt extrusion. As warm water is a main source to trigger the degradation and recycling, the proposed mechanism might be a more sustainable and cost-effective approach than the use of toxic and expensive organic solvents in recycling of e-waste made of multi-components. These new biodegradable, recyclable, conductive, flexible, and printable material can be applied across many electronic devices to serve as a cornerstone for the development of eco-friendly, recyclable electronics.

Schematic 1. The recycling mechanism of the printed circuits using RHP/BC-Lipase$_{np}$ nanoclusters. **(a)** Flexible electronic circuits fabricated by 3D printing or direct ink writing. The circuits can be disintegrated in warm water, and the separated fillers can be recollected. **(b)** The conductive ink including functional fillers, PCL, and RHP/BC-Lipase$_{np}$. The binder,

PCL represented by gray chains, degrades through chain scission depolymerization in warm water. RHP/BC-Lipase$_{np}$ includes BC-Lipase (green), enzyme protectant (RHPs) highlighting the hydrophilic (blue) and the hydrophobic (pink) segments, and impurities (gray spheres).

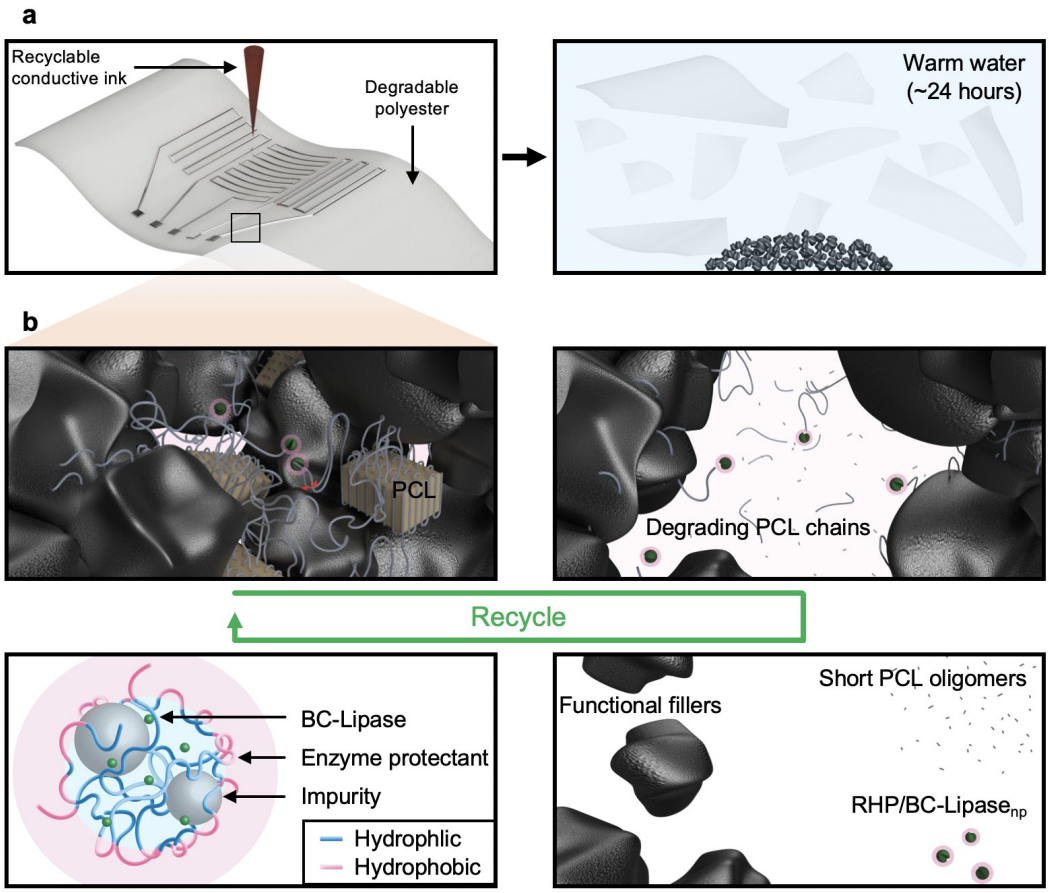

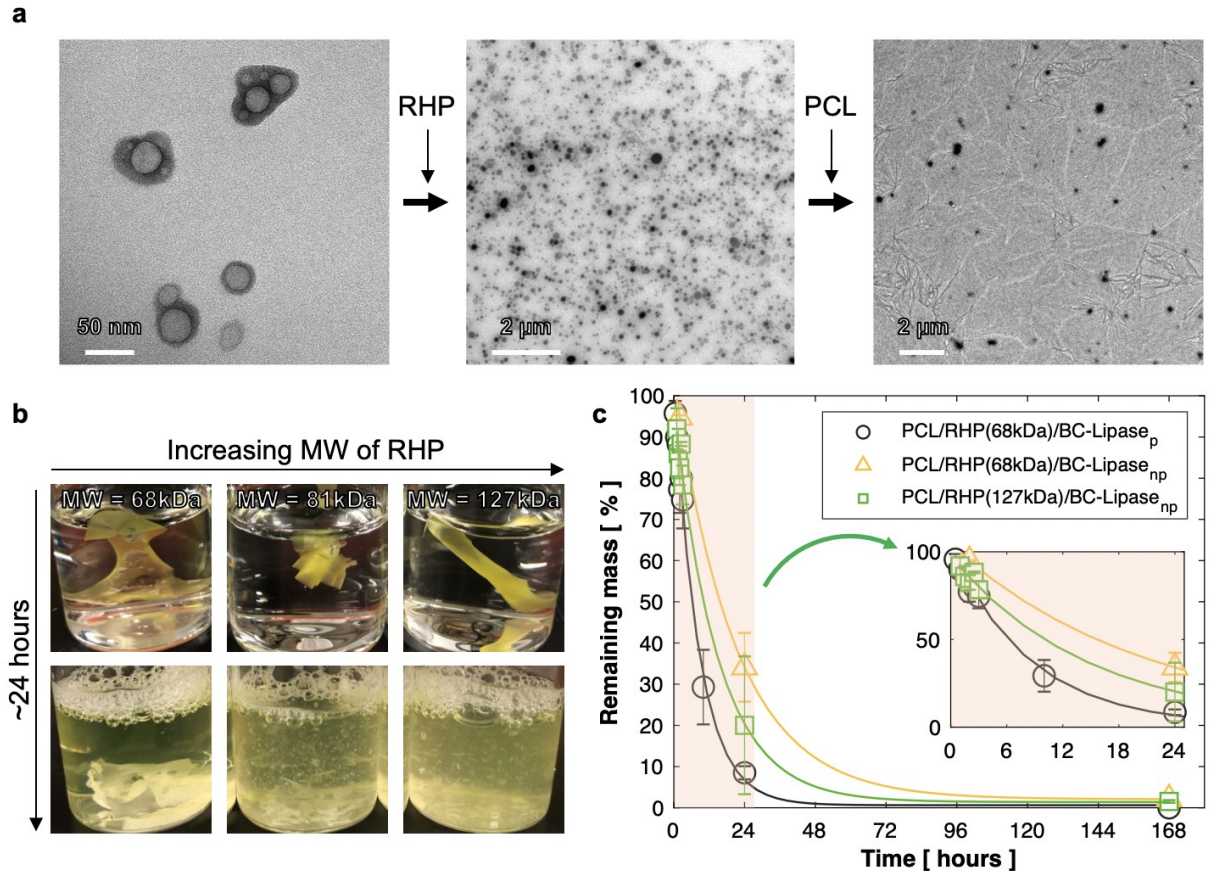

Figure 1. The conductive ink with nanoscopically-dispersed RHP/BC-Lipase$_{np}$ with the degradation performance affected by the molecular weight of the RHPs. TEM images of **(a)** the non-purified enzyme complex in water, RHP/BC-Lipase$_{np}$, and PCL/RHP/BC-Lipase$_{np}$. **(b)** The degradation results for PCL/RHP/BC-Lipase$_{np}$ with the different molecular weights of RHPs (68 kDa, 81 kDa, and 127 kDa). The fluorescently labeled BC-Lipase$_{np}$ was used for color contrast. **(c)** Degradation profiles of PCL with purified BC-Lipase (PCL/RHP(68kDa)/BC-Lipase$_p$) and with non-purified BC-Lipase (BC-Lipase$_{np}$) that was embedded with either 68 kDa or 127 kDa RHP. Three films of each sample and time were evaluated for analysis.

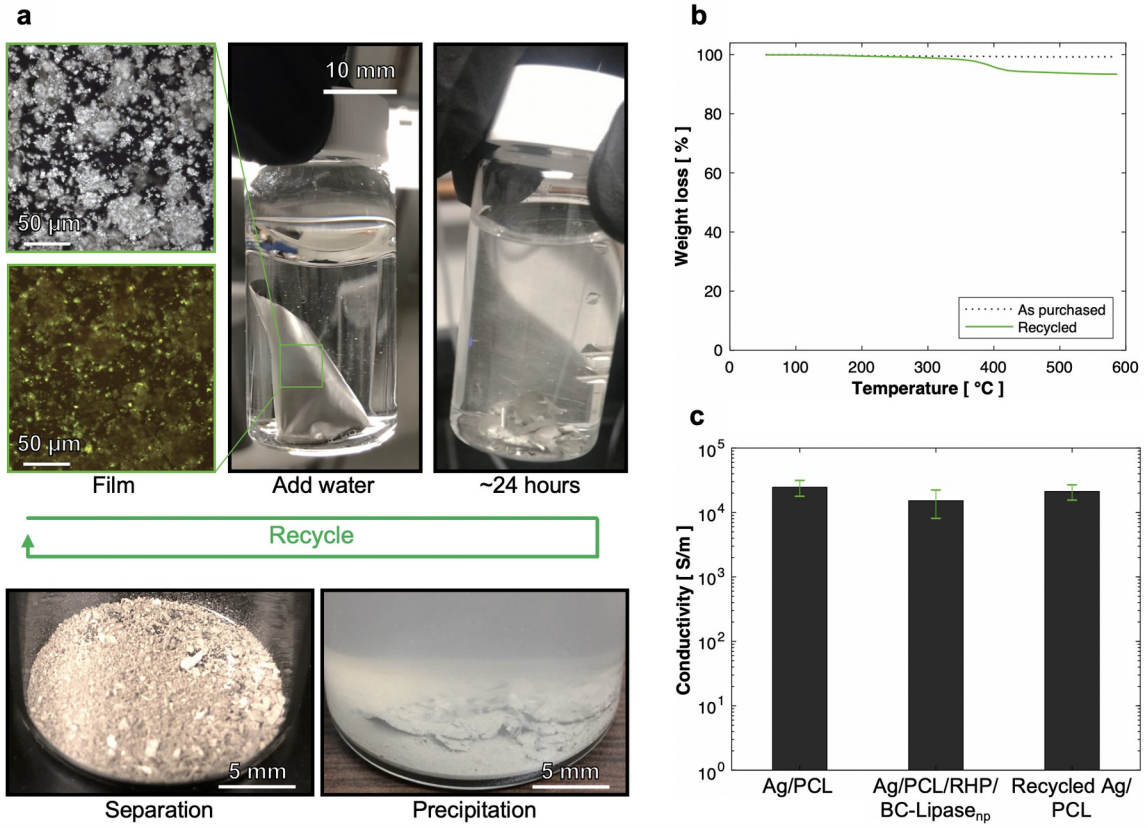

Figure 2. E-waste recycling. **(a)** Recycling process of metal fillers by enzyme-catalyzed degradation. A dry-cast Ag/PCL/RHP/BC-Lipase$_{np}$ film was placed in a warm buffer (37˚C). Optical microscope image of the ink (~80 wt.% of Ag flakes) and fluorescence microscope image of the ink with fluorescently labeled BC-Lipase$_{np}$. After the degradation (~24 hours), Ag flakes were precipitated and recollected for recycling. **(b)** TGA of the recycled and as purchased Ag flakes. **(c)** Comparison of the electrical conductivity of composites with and without enzyme clusters and with recycled Ag flakes (78.9 wt.%).

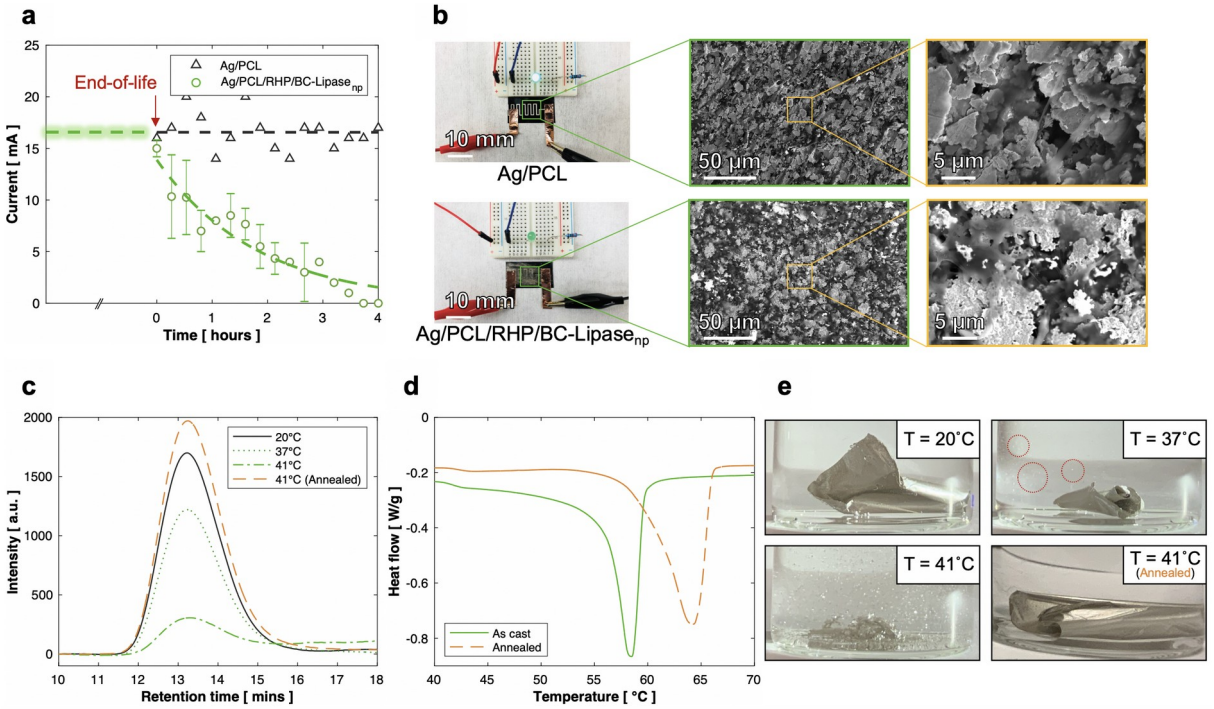

Figure 3. Degradation tests under electrical voltage. **(a)** The enzymatic degradation under a 5 V potential of Ag/PCL/RHP/BC-Lipase$_{np}$ over time, triggered by warm water. The circuits are conductive under ambient conditions at room temperature for 1 month or under water (20˚C). When the degradation begins by increasing the water temperature to 37˚C, the measured electrical currents decrease as the PCL degrades, showing that the activity of BC-Lipase is not compromised under an electrical potential. Statistical values were measured from four independent measurements. **(b)** SEM images of the printed circuits with and without RHP/BC-Lipase$_{np}$ after the degradation test. **(c)** GPC results of Ag/PCL/RHP/BC-Lipase$_{np}$ and the thermally annealed film after degradation (~24 hours). The films were degraded as a function of water temperature (20, 37, and 41˚C). Mass loss results, estimated by integrating GPC peaks, show that the degradation rate is proportional to degradation temperature. **(d)** DSC results of the as cast and annealed films. The thermal annealing process increased the crystallinity from 49.8% to 55.1%, as the melting enthalpy of 100% crystalline PCL was taken as 151.7 J/g.[18] **(e)** The films in water after the degradations at various temperatures (~24 hours). Increased mass loss was observed with increasing temperature in as cast films, whereas annealed films remained intact even at 41˚C. Red circles indicate the silver particles dispersed in water.

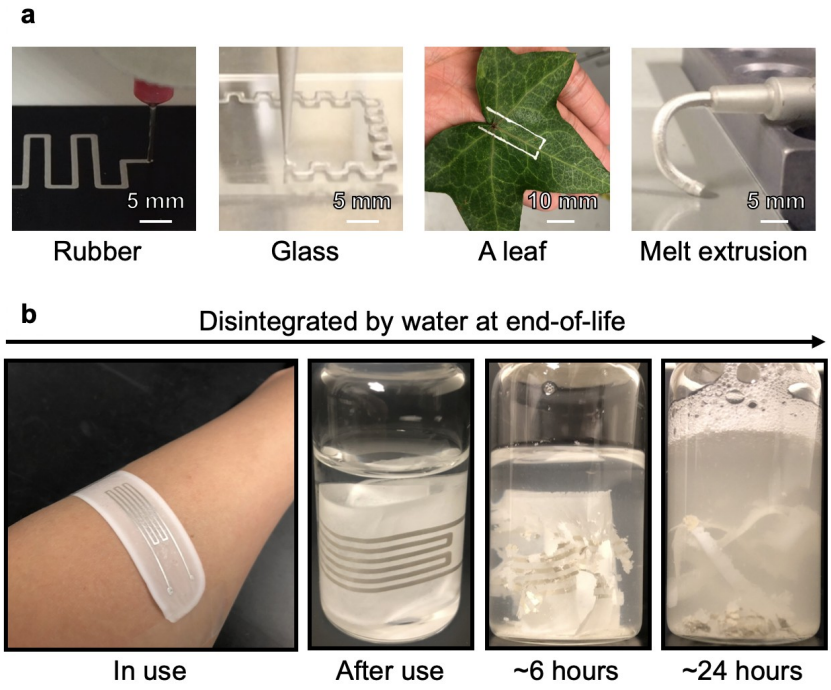

Figure 4. 3D printing applications. **(a)** The ink printed on rubber, glass, and a leaf using melt extrusion. Ag flakes and RHP/BC-Lipase$_{np}$ were mixed in the PCL melt (~60˚C) and then the mixture was extruded from a heated nozzle. **(b)** The ink was printed on a PCL/RHP/BC-Lipase$_{np}$ substrate. The printed circuit disintegrates in warm water at end-of-life.

Experimental Section/Methods

Materials:

Polycaprolactone (PCL) (80,000 g/mole, PDI < 2) and Amano PS Lipase from Burkholderia cepacia were purchased from Sigma-Aldrich® and Ag flakes from Inframat®. The enzyme was dissolved in water and stored at -20˚C until use. Toluene (HPLC grade, > 99.8% purity) and the salts to make the phosphate buffer (pH = 7.4) were purchased from Fisher Chemical®. PCL (20,000 g/mole, PDI<2) was used for the melt extrusion demonstration. The buffer was prepared with milli-Q water, potassium chloride, and sodium chloride.

Methods:

Ink preparation: The random heteropolymer (RHP) was designed with four different monomers matching the chemically heterogeneous enzyme surfaces and synthesized as previously reported.[9b] The synthesized RHP was dissolved in water. Both BC-Lipase$_{np}$ and RHP water solutions were mixed together in room temperature for 5 minutes. The ratio RHP/ BC-Lipase$_{np}$ was 2:1 by mass. The RHP/BC-Lipase$_{np}$ solution was dried *in vacuo* overnight. The dried RHP/BC-Lipase$_{np}$ was mixed with PCL-Toluene solution (100 mg/mL) and silver flakes for 5 minutes to produce the proper viscosity of the solution to be printed, and to allow for quick solvent evaporation. The mass ratio of RHP/BC-Lipase$_{np}$ and Ag/PCL ink was 98:2.

Direct ink writing (3D Printing): The Ag/PCL/RHP/BC-Lipase$_{np}$ ink was printed at room temperature with a three-axis motion-controlled stage (Aerotech) with the print paths generated with 3D robotic deposition software (Robocad 3.0). The diameter of the paths was set to 150-600 μm controlled by the size of the printing tips (EFD precision tips, EFD, East

Providence, RI); the extrusion of inks was controlled with an additional motor attached to the syringe. Toluene was selected as the printing solvent for its boiling point (110.6˚C) in order to prevent clogging of the nozzle which can introduce defects or particle aggregations during the printing process.

Structural characterization: Transmission electron microscopy (TEM) imaging was performed on a FEI Tecnai 12 microscope operating at a 120 kV accelerating voltage. Scanning electron microscopy (SEM) imaging was performed on a Hitachi S-5000 microscope. Scanning transmission electron microscopy-energy dispersive X-ray spectroscopy (STEM-EDS) was performed at the National Center for Electron Microscopy (NCEM) of the Molecular Foundry by using a FEI TitanX 60-300 microscope operated at 200 kV. The Bruker windowless EDS detector with a solid angle of 0.7 steradians enables high count rates with minimal dead time.-The data were visualized with Esprit 1.9. Gel permeation chromatography (GPC) measurements were run using a total concentration of 2 mg/mL of the remaining Ag/PCL/RHP/BC-Lipase$_{np}$ film after the degradation (24 hours) and a by-product in THF. 20 μL of solution was injected into an Agilent PolyPore 7.5 × 300 mm column.

Mechanical testing characterization: Uniaxial tensile tests were performed on a screw-driven mechanical testing machine (Instron-5933, Norwood, MA) with a 2 kN load cell. 300 μm films were cut into dog-bone samples with an ASTM D1708 cutting die; the specimen gauge lengths were set at 22 mm with the longitudinal strain calculated from the crosshead displacement. Testing was carried out at room temperature at a displacement rate of 10 mm/min. At least five samples of each condition were tested. Lap-shear tests were performed at a rate of 1 mm/min with two styrene-ethylene-butylene-styrene elastomer substrates (5 × 10 × 0.1 mm) and the ink (5 × 5 mm) in between them after ~12 hours of degradation.

Thermal characterization: Differential scanning calorimetry (DSC) (TA Instruments) measurements were performed at temperatures at 20˚C to 70˚C under nitrogen gas with a rate

of 2˚C/min. Thermogravimetric analysis (TGA) (TA Instruments) measurements were performed at 25˚C to 600˚C with a rate of 20˚C/min in a nitrogen atmosphere.

Conductivity measurements: A constant electrical potential of 5 V was applied using a DC power supply (E3612A, Agilent) and the buffer was heated to 37˚C using a silicon oil bath. The buffer level was kept constant with condensation controlled using a long tube glass. The recycled silver flakes were washed once with toluene and dried at room temperature before measurements.

Statistical analysis: The presented data were not pre-processed for statistical analysis. Statistical values, such as mean and standard deviations, were calculated from more than three independent experiments. MATLAB and image-J were used for the analysis.

Supporting Information

Supporting Information is available from the Wiley Online Library or from the author.

Acknowledgements

This work was supported by the U.S. Department of Energy, Office of Science, Office of Basic Energy Sciences, Materials Sciences and Engineering Division (DOE-BES-MSE) under Contract DE-AC02-05-CH11231, through the Organic–Inorganic Nanocomposites KC3104 program. J.K. was supported by at UC Berkeley by a Jane Lewis Fellowship. T.X. conceived the idea and guided the project. J.K., C.D. and T.X. performed material characterization experiments, scalability studies, and analyzed degradation rates. J.K., A.D., and M.M. 3D printed the electronic circuits. J.K. and C.D. performed electron microscopy experiments and gel permeation chromatography characterizations. C.D. and L.M performed transmission electron microscopy and energy-dispersive X-ray spectroscopy. J.K. and R.O.R. analyzed mechanical properties. P.K., A.H., and I.J. synthesized and characterized the RHPs. **Competing interests**: T.X., C.D., and J.K. filed a patent disclosure. A.H. is the founder and CEO of Intropic Materials.

References

[1] J. R. Jambeck, R. Geyer, C. Wilcox, T. R. Siegler, M. Perryman, A. Andrady, R. Narayan, K. L. Law, *Science* **2015**, 347, 768.

[2] A. Islam, T. Ahmed, M. R. Awual, A. Rahman, M. Sultana, A. A. Aziz, M. U. Monir, S. H. Teo, M. Hasan, *J. of Clean. Prod.* **2020**, 244, 118815.

[3] P. Kiddee, R. Naidu, M. H. Wong, *Waste Manag.* **2013**, 33, 1237.

[4] a) A. Kumar, M. Holuszko, D. C. R. Espinosa, *Conserv. Recycl.* **2017**, 122, 32; b) J. Cui, L. Zhang, *J. Hazard. Mater.* **2008**, 158, 228.

[5] a) N. X. Williams, G. Bullard, N. Brooke, M. J. Therien, A. D. Franklin, *Nature Electron.* **2021**, 4, 261; b) W. B. Han, J. H. Lee, J.-W. Shin, S.-W. Hwang, *Adv. Mater.* **2020**, 32, 2002211.

[6] S.-W. Hwang, H. Tao, D.-H. Kim, H. Cheng, J.-K. Song, E. Rill, M. A. Brenckle, B. Panilaitis, S. M. Won, Y.-S. Kim, Y. M. Song, K. J. Yu, A. Ameen, R. Li, Y. Su, M. Yang, D. L. Kaplan, M. R. Zakin, M. J. Slepian, Y. Huang, F. G. Omenetto, J. A. Rogers, *Science* **2012**, 337, 1640.

[7] a) S. W. Hwang, S. K. Kang, X. Huang, M. A. Brenckle, F. G. Omenetto, J. A. Rogers, *Adv. Mater.* **2015**, 27, 47; b) C. W. Park, S. K. Kang, H. L. Hernandez, J. A. Kaitz, D. S. Wie, J. Shin, O. P. Lee, N. R. Sottos, J. S. Moore, J. A. Rogers, *Adv. Mater.* **2015**, 27, 3783; c) H. L. Hernandez, S. K. Kang, O. P. Lee, S. W. Hwang, J. A. Kaitz, B. Inci, C. W. Park, S. Chung, N. R. Sottos, J. S. Moore, *Adv. Mater.* **2014**, 26, 7637.

[8] J. Shim, J. A. Rogers, S. Kang, *Mat. Sci. and Eng. R Rep.* **2021**, 145, 100624.

[9] a) C. DelRe, B. Chang, I. Jayapurna, A. Hall, A. Wang, K. Zolkin, T. Xu, *Adv. Mater.* **2021**, 33, 2105707; b) B. Panganiban, B. Qiao, T. Jiang, C. DelRe, M. M. Obadia, T. D. Nguyen, A. A. Smith, A. Hall, I. Sit, M. G. Crosby, *Science* **2018**, 359, 1239; c) C. DelRe, Y. Jiang, P. Kang, J. Kwon, A. Hall, I. Jayapurna, Z. Ruan, L. Ma, K. Zolkin, T. Li, C. D. Scown, R. O. Ritchie, T. P. Russell, T. Xu, *Nature* **2021**, 592, 558.

[10] D. Stauffer, A. Aharony, *Introduction to percolation theory*, Taylor & Francis, London, UK **1994**.

[11] a) J. Kwon, K. Evans, M. Le, D. Arnold, M. E. Yildizdag, T. Zohdi, R. O. Ritchie, T. Xu, *ACS Appl. Mater. Interfaces* **2020**, 12, 8687; b) A. D. Valentine, T. A. Busbee, J. W. Boley, J. R. Raney, A. Chortos, A. Kotikian, J. D. Berrigan, M. F. Durstock, J. A. Lewis, *Adv. Mater.* **2017**, 29, 1703817.

[12] A. Cholewinski, P. Si, M. Uceda, M. Pope, B. Zhao, *Polymers* **2021**, 13.

[13] J. Si, Z. Cui, Q. Wang, Q. Liu, C. Liu, *Carbohydr. Polym.* **2016**, 143, 270.

[14] D. Liu, G. Sui, Y. Dong, *Electrospun Polymers and Composites*, Woodhead Publishing **2021**, p. 147-178.

[15] S. Y. Ho, G. S. Mittal, J. D. Cross, *J. Food Eng.* **1997**, 31, 69.

[16] D. Toker, D. Azulay, N. Shimoni, I. Balberg, O. Millo, *Phys. Rev. B* **2003**, 68, 041403.

[17] S. Zhang, E. Forssberg, *Conserv. Recycl.* **1997**, 21, 247.

[18] A. Wurm, E. Zhuravlev, K. Eckstein, D. Jehnichen, D. Pospiech, R. Androsch, B. Wunderlich, C. Schick, *Macromolecules* **2012**, 45, 3816.

ToC Text: The recyclability and sustainability of printed electronics have important design aspects in reducing the costs and environmental burden of electronic wastes. Enzymatic degradation can be considered, but resource-intensive purification of enzymes limits scalability, and their stability is uncertain under electrical voltage and long-term storage. By employing the customized enzyme protectant, the ink can be disintegrated and recycled in warm water.

J. Kwon, C. DelRe, P. Kang, A. Hall, D. Arnold, I. Jayapurna, L. Ma, M. Michalek, R. O. Ritchie, and T. Xu*

Conductive ink with circular life cycle for printed electronics

ToC figure (55 mm broad × 50 mm high):

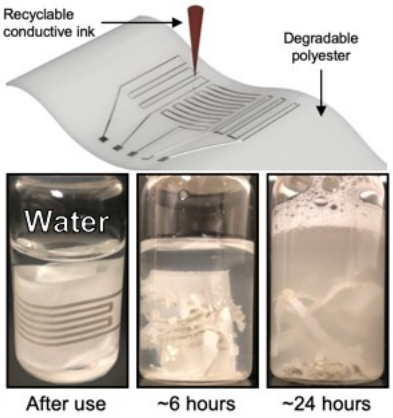

Supporting Information

Conductive ink with circular life cycle for printed electronics

Junpyo Kwon, Christopher DelRe, Philjun Kang, Aaron Hall, Daniel Arnold, Ivan Jayapurna, Le Ma, Matthew Michalek, Robert O. Ritchie, and Ting Xu*

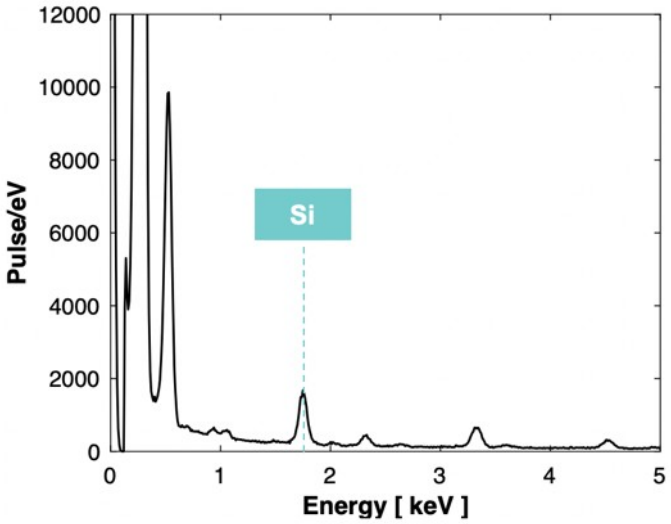

Figure S1. STEM-EDS spectrums of commercial, non-purified BC-Lipase blends.

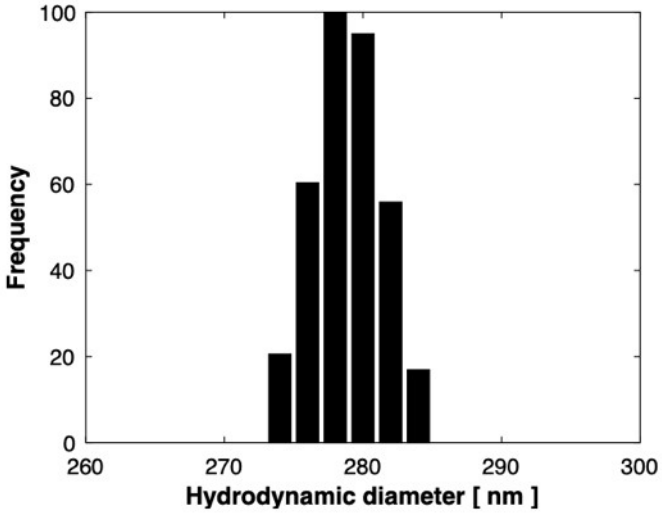

Figure S2. The hydrodynamic diameter of RHP(62kDa)/BC-Lipase$_{np}$ in toluene measured by DLS.

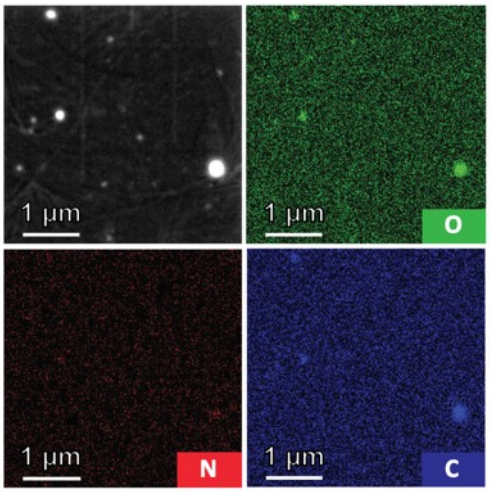

Figure S3. STEM-EDS images of PCL/RHP/BC-Lipase$_{np}$ with oxygen, nitrogen, and carbon distributions.

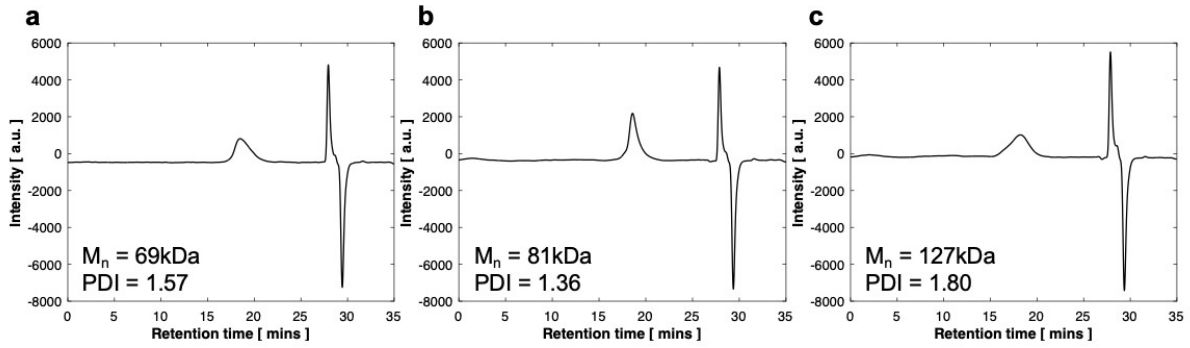

Figure S4. GPC traces of the different molecular weights of RHPs. Poly(methylmethacrylate) standards were used for calibration. The measured MWs are 69 kDa, 81 kDa, and 127 kDa with PDIs, 1.57, 1.36, and 1.80, respectively.

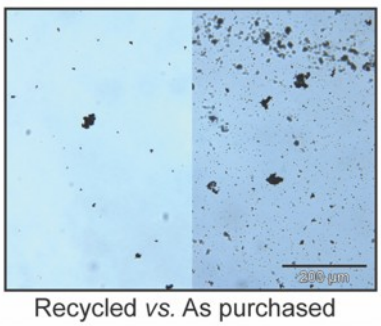

Figure S5. Comparisons of recycled and as purchased Ag flakes. Optical images of the (left) recycled Ag flakes, and (right) as purchased flakes.

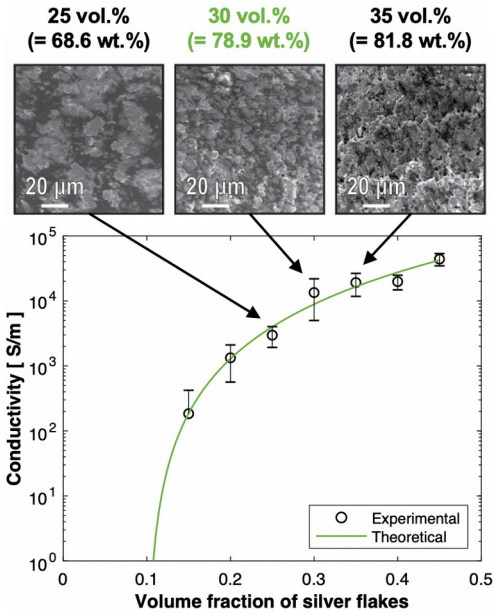

Figure S6. SEM images of PCL/Ag/RHP/BC-Lipase$_{np}$ with different volume fractions of Ag flakes (25, 30, and 35 vol.%). The electrical conductivity of the ink changes as a function of the volume fraction of Ag flakes. The solid line is the fitted curve based on the experimental results with percolating network theory, $\sigma^{*} = \sigma_0 (v_f - v_c)^s$, where σ^* and σ_0 are the bulk conductivity of Ag/PCL/RHP/BC-Lipase$_{np}$ and silver flakes and where v_c the critical volume fraction at percolation, and s is the power law exponent. The calculated values of σ_0, v_c, and s are 7.9 $\times$ 10^5 S/m, 0.1, and 2.79, respectively. The volume fractions of Ag flakes can be converted to the corresponding weight percentages based on the densities of PCL, Ag flakes, RHP, and BC-Lipase$_{np}$. More than five samples were evaluated.

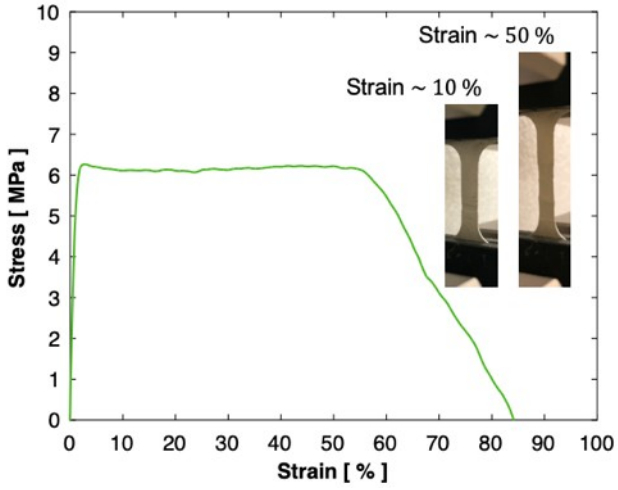

Figure S7. Uniaxial tensile engineering stress-strain curve of Ag/PCL/RHP/BC-Lipase$_{np}$.

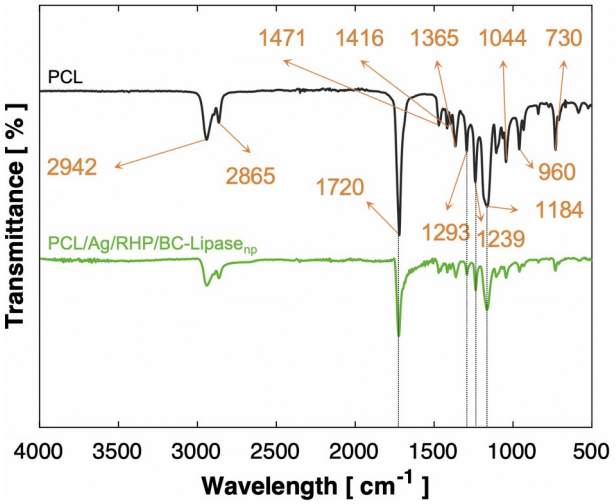

Figure S8. FT-IR spectra of PCL and PCL/Ag/RHP/BC-Lipase$_{np}$.

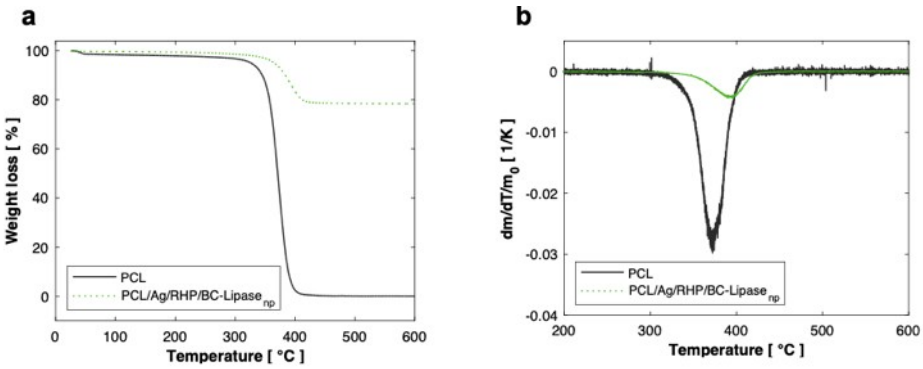

Figure S9. TGA results of **(a)** PCL and Ag/PCL/RHP/BC-Lipase$_{np}$ and **(b)** their derivative TGA curves.

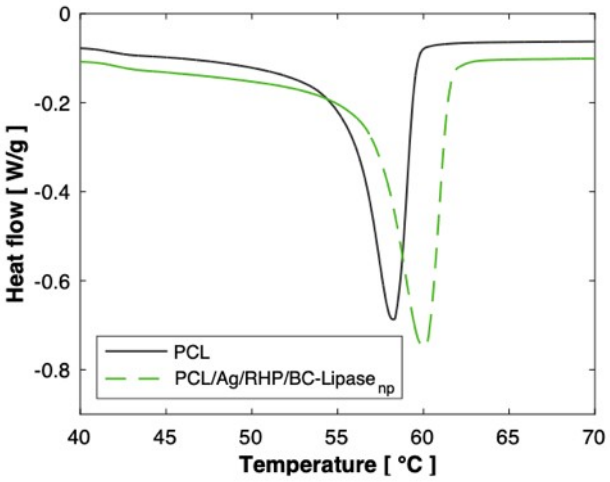

Figure S10. DSC results of PCL and PCL/Ag/RHP/BC-Lipase$_{np}$.

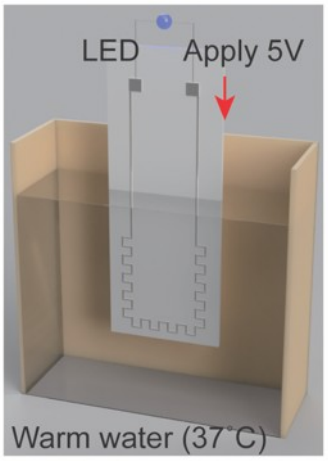

Figure S11. Degradation experimental set-up.

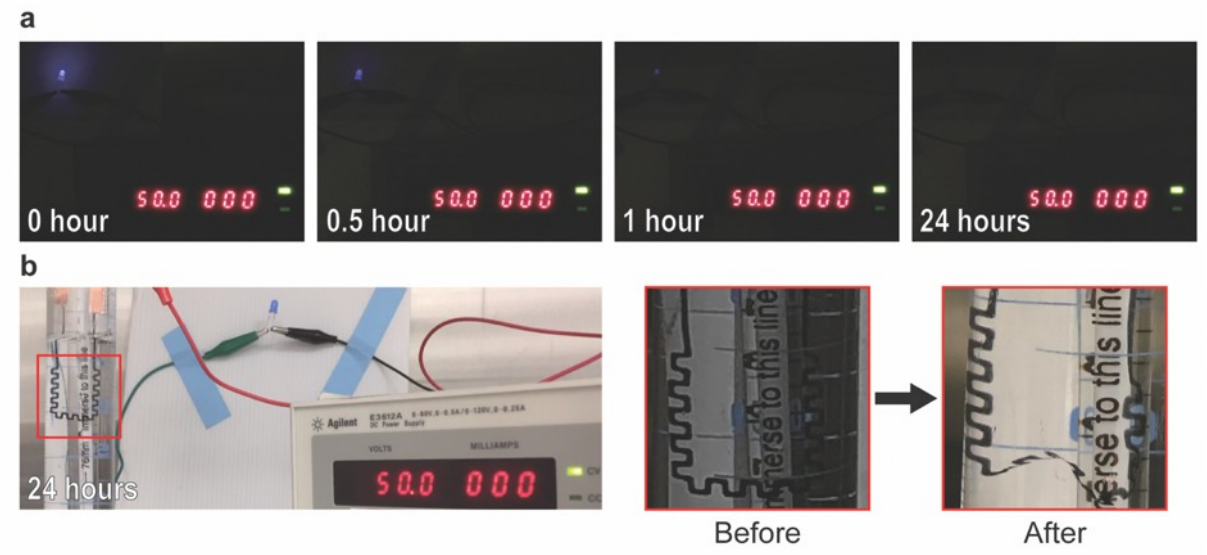

Figure S12. Degradation tests with different filler types. **(a)** The degradation test of the printed circuits made of PCL/Carbon black/RHP/BC-Lipase$_{np}$ with 50 V. **(b)** The circuit was delaminated from a glass substrate after the degradation.

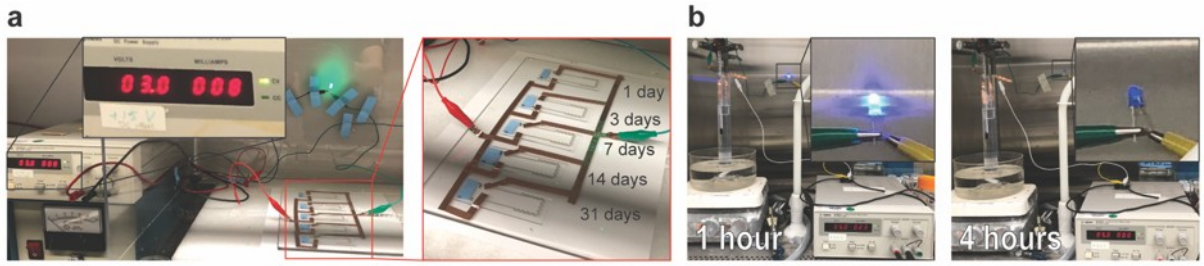

Figure S13. Enzyme stability tests under electrical voltage. **(a)** The circuits were fabricated ~7 months before the test, and a voltage (3 V) was applied for 1, 3, 7, 14, and 31 days, respectively. **(b)** All PCL/Ag/RHP/BC-Lipase$_{np}$ circuits were degraded within 4 hours in warm water under 5 V.

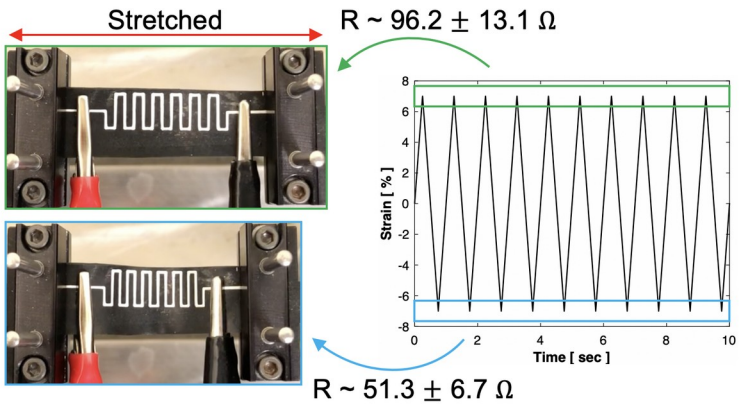

Figure S14. The flexibility of the printed circuits in cyclic stretch test (1,000 cycles) showing the different conductivity under mechanical loading. The strain was measured by the initial length of the substrate.

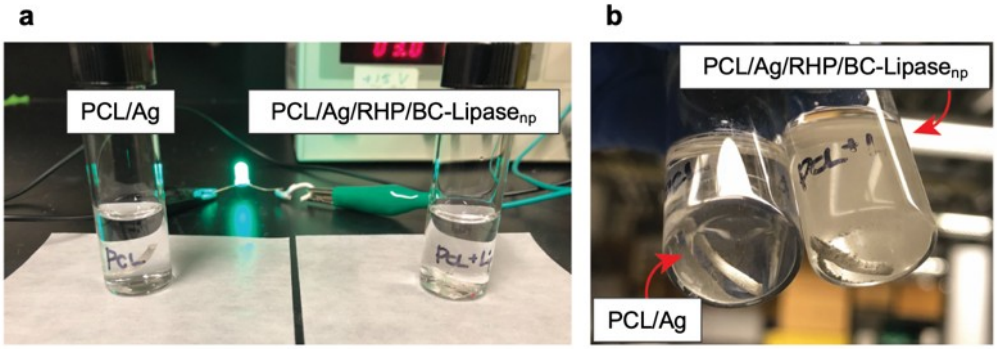

Figure S15. (a) The extruded samples showing electrical conductivity in a warm water before the degradation. **(b)** The melt-extruded PCL/Ag/RHP/BC-Lipase$_{np}$ was degraded at 37˚C for 3 days, as compared to the non-degraded Ag/PCL.

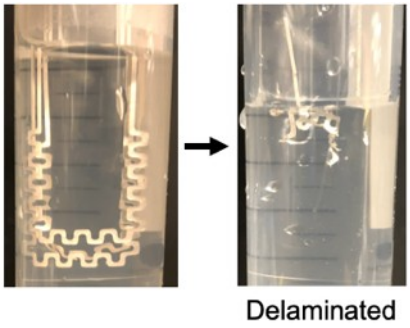

Figure S16 The circuits are easily detached from the substrates after degradation.

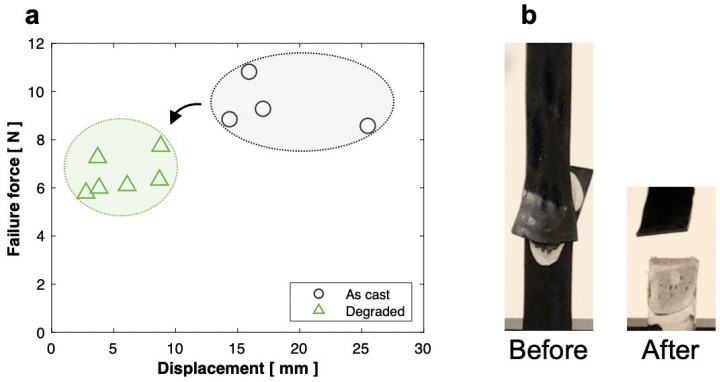

Figure S17 (a) The failure force measured by the lap-shear adhesion test using PCL/Ag, PCL/Ag/RHP/BC-Lipase$_{np}$ before and after degradation. All failures were cohesive failures. **(b)** Comparison of the adhesion force of the ink before and after the degradation.

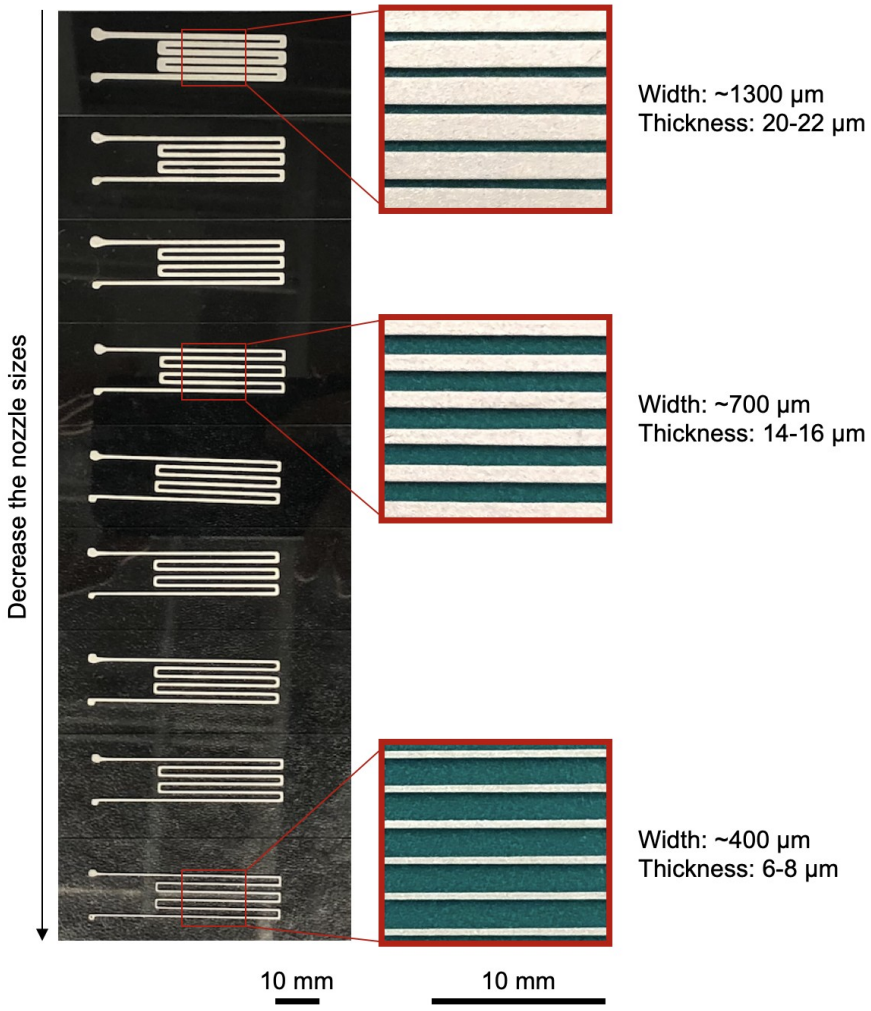

Figure S18 The printed circuits with different widths and thicknesses obtained by changing the nozzle size.

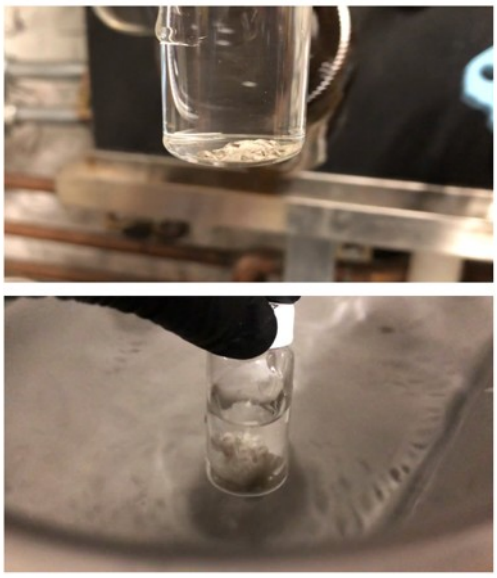

Video S1. Ag/PCL/RHP/BC-Lipase$_{np}$ degraded in warm water.

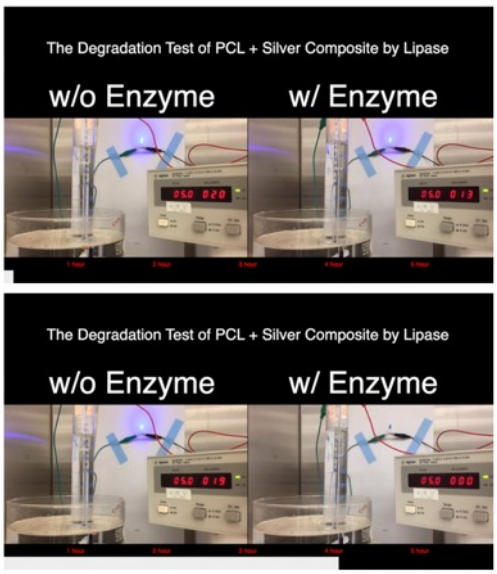

Video S2. Degradation tests of the conductive ink under an electrical voltage (5 V) with and without RHP/BC-Lipase$_{np}$.

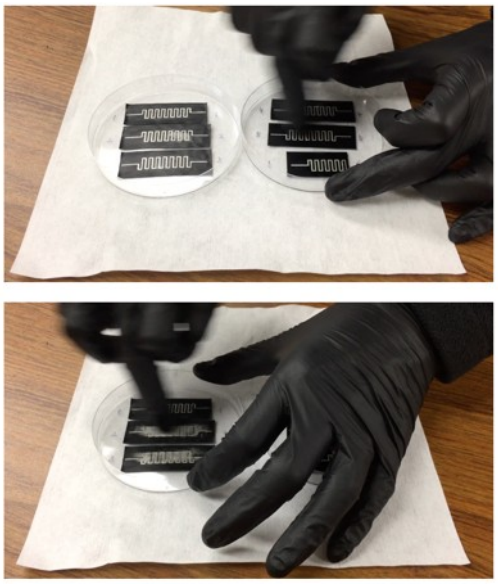

Video S3. Comparison of the degradation of the printed circuits with and without RHP/BC-Lipase$_{np}$.